Kongunadu Research Journal 13 (1):48-57, 2026 ISSN 2349-2694, All Rights Reserved,

Publisher: Kongunadu Arts and Science College, Coimbatore. https://krjournal.com/index.php/krj/article/view/742

DOI:10.26524/krj.2026.8

RESEARCH ARTICLE

ELECTRO-OSMOSIS INDUCED PERISTALTIC FLOW OF EYRING-POWELL NANOFLUID THROUGH A TAPERED ASYMMETRIC CHANNEL WITH THERMAL RADIATION EFFECTS

Asha S. Kotnurkar [a,*], Susama Junjappanavar [b]

[a,b] Department of studies in Mathematics, Karnatak University, Dharwad-580003, Karnataka, India.

[*]**Corresponding author E-mail ID: ashask@kud.ac.in**

Abstract

In the current analysis, the peristaltic transport of an Eyring–Powell nanofluid through a tapered asymmetric channel is explored with particular attention to electro-osmosis and thermal radiation effects. The mathematical model is developed within the framework of the long-wavelength along with low Reynolds number approximations, which allow considerable simplification without losing the essential physics. By employing appropriate non-dimensional variables, the fluid transport problem is reformulated as a coupled system of nonlinear partial differential equations. Analytical expressions for the velocity, temperature, and nanoparticle volume fraction are derived to describe the flow characteristics. The study further highlights the influence of key parameters including electro-osmotic parameter, fluid parameters, local nanoparticle Grashof number, Helmholtz–Smoluchowski velocity, local thermal Grashof number on the velocity profile. The graphical illustrations emphasize the impact of major physical parameters namely Brownian motion parameter, Prandtl number, thermophoresis parameter and thermal radiation parameter on temperature and nanoparticle volume fraction variation. The findings of this study hold significant relevance for biomedical micro devices, where they can facilitate precise regulation of chemical and biological fluids and further contribute to advancements in cancer therapy and targeted drug delivery.

Keywords: Peristaltic Flow, Electro-osmosis, Eyring-Powell Nanofluid, Thermal Radiation, Tapered Asymmetric Channel

1. INTRODUCTION

A continuous wave of area compression or expansion moving along its length is called peristalsis, and it is a process of fluid transfer. The Greek term peristallein is the source of the Latin word peristalsis. Pumping industrial, physiological, and other types of fluids from one location to another is accomplished by the peristalsis process. Along with numerous industrial and biomedical applications, this phenomenon manifests in various physiological processes such as food transport through the esophagus, bile flow in the bile duct, ciliary transport, chyme propulsion in the gastrointestinal tract and spermatozoa migration within the cervical canal [1]. It is also widely used in industries where close contact with boundaries is forbidden. The food and beverage business, cell separation, mining, medical sector, the finger, hose, and roller pumps are a few examples.

The idea of peristaltic flow was first proposed by Latham [2] in 1966. Subsequently, extensive analytical, computational, and experimental studies on peristaltic transport of different fluids came to be reported under diverse conditions, addressing both mechanical and physiological contexts [3]. Later research on peristaltic flow in different geometries was carried out by Shapiro et al. [4] and Jaffrin et al. [5]. Peristalsis motion has been the subject of numerous empirical studies for fluid flow in various channels. The peristaltic movement of nanofluid in presence of Jeffrey fluid's gold nanoparticles was examined by Asha et al. [6–7]. Additionally, the peristalsis of nanofluid through deformable channel involving double diffusion was the topic of Aamir et al. [8].

The process by which an applied electric potential creates mobility in an ionized solution (electrolyte) confined in a channel is known as the mechanism of electro-osmosis. In electro-osmosis flow, a solid surface that comes into contact with the electrolyte solution is charged. In this process, opposing ions are drawn to the surface by the electric potential, which causes an electron double layer (EDL) to form. Fluid motion results from the Coulomb force, which is created when an ionic solution is exposed to an external electric field. This phenomenon is used to control fluid flow through tiny channels in bio microfluidic devices. Bio microfluidics devices that employ electro-osmosis and EDL principles include lab-on-chip and peristaltic micro pump. A crucial element in the advancement of DNA analysis methods is capillary electrophoresis. Consequently, peristaltic pumping-influenced electro-osmotically flowing fluid may be utilized in DNA analysis, that can subsequently be applied to DNA sequencing, DNA length measurement, and the identification of genetic diseases [9]. Recent research on electro-osmosis can be found in [10-12].

To evaluate the heat transfer rate from one area to another in a variety of conductive and convective processes, recent studies have focused more on thermal convective fluxes. The temperature variation at the movement area determines the thermal energy. However, with thermal radiation, the absolute temperature difference determines how much energy is transferred between two bodies. There are several uses for thermal radiation in the biomedical sector. The impact of thermal radiation became an important study area due to its use in biomedicine and medical therapy.

In 1944, Eyring and Powell proposed the Eyring–Powell model, a distinctive non-Newtonian fluid concept [13]. This model is very useful for recovering viscous nanofluid observations accurately at both low and high shear rates. This model's complicated mathematical description in a flexible curving channel may prevent researchers from studying nanoparticles liable to Eyring-Powell fluid [14].

This study investigates the influence of thermal radiation and electro-osmosis on the peristaltic transport of an Eyring–Powell nanofluid within a tapered asymmetric channel, subject to appropriate boundary conditions. The governing equations are formulated in a wave frame of reference and simplified through the assumptions of long wavelength and low Reynolds number. Employing the Homotopy Perturbation Sumudu Transformation Method, closed-form solutions for velocity, temperature, and nanoparticle concentration are derived from the dimensionless nonlinear partial differential equations [15]. To interpret the impact of relevant physical parameters, graphical illustrations are presented and discussed.

2. MATHEMATICAL FORMULATION OF THE PROBLEM

This study focuses on the peristaltic motion of a non-Newtonian fluid under the influence of electro-osmosis along a tapered asymmetric channel. The physical model is formulated in terms of axial ($\overline{X}$) and transverse ($\overline{Y}$) coordinates, where the respective velocity factors $\overline{U}$ and $\overline{V}$ are defined. The channel boundaries are positioned at $\overline{Y}=\overline{H_1}$ (left) and $\overline{Y}=\overline{H_2}$ (right) as illustrated in Fig.1. The driving mechanism of the flow originates from sinusoidal waves traveling along the irregular asymmetric channel walls with a uniform propagation speed c. The mathematical description of the wall configuration is formulated as below [16].

$$\overline{H_1}(\overline{X},\overline{t}) = -d - m'\overline{X} - a\sin\left(\frac{2\pi}{\lambda}(\overline{X}-c\overline{t})+\phi\right), \tag{2.1}$$

$$\overline{H_2}(\overline{X},\overline{t}) = d + m'\overline{X} + b\sin\left(\frac{2\pi}{\lambda}(\overline{X}-c\overline{t})\right) \tag{2.2}$$

where a,b,d,c,m',λ,ϕ are the left and right-wall amplitudes, channel half-width, propagation velocity of the wave, tapering (non-uniformity) parameter, wavelength, and phase shift respectively. Furthermore, a,b,d,ϕ satisfy the condition $a^2+b^2+2ab\cos(\phi)\le(2d)^2$.

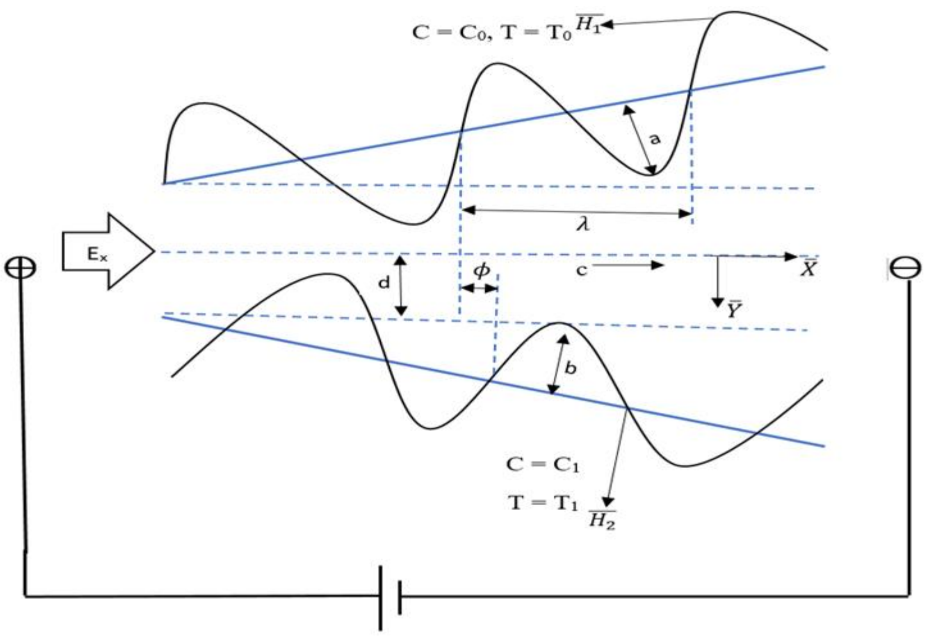

Fig. 1. Schematic diagram of a two-dimensional tapered asymmetric channel

Fluid Model:

Extra stress tensor $\hat{S}$ of Eyring-Powell fluid model [17] is

$$\hat{S} = \mu\nabla\overline{V} + \frac{1}{\beta}\sinh^{-1}\left(\frac{1}{c^*}\nabla\overline{V}\right), \tag{2.3}$$

where β and c^* are the fluid parameters, μ is viscosity,

$$\sinh^{-1}\left(\frac{1}{c^*}\nabla\overline{V}\right) \approx \frac{1}{c^*} - \frac{1}{6}\left(\frac{1}{c^*}\nabla\overline{V}\right)^3, \left|\frac{1}{c^*}\nabla\overline{V}\right| \le 1 \tag{2.4}$$

The suitable equations for flow of the present problem are provided by:

Continuity Equation:

$$\frac{\partial\overline{U}}{\partial\overline{X}} + \frac{\partial\overline{V}}{\partial\overline{Y}} = 0 \tag{2.5}$$

Momentum Equation:

$$\rho_f\left(\frac{\partial\overline{U}}{\partial\bar{t}} + \overline{U}\frac{\partial\overline{U}}{\partial\overline{X}} + \overline{V}\frac{\partial\overline{U}}{\partial\overline{Y}}\right) = -\frac{\partial\overline{P}}{\partial\overline{X}} + \left(\mu + \frac{1}{\beta c^*}\right)\left(\frac{\partial^2\overline{U}}{\partial\overline{X}^2} + \frac{\partial^2\overline{U}}{\partial\overline{Y}^2}\right)$$
$$-\frac{1}{2\beta c^{*3}}\left(\frac{\partial\overline{U}}{\partial\overline{X}} + \frac{\partial\overline{U}}{\partial\overline{Y}}\right)^2\left(\frac{\partial^2\overline{U}}{\partial\overline{X}^2} + \frac{\partial^2\overline{U}}{\partial\overline{Y}^2}\right) + \rho_e E_x$$
$$+\rho_f g\beta_T(\overline{T} - \overline{T}_0) + (\rho_p - \rho_f)g\beta_c(\overline{C} - \overline{C}_0) \tag{2.6}$$

$$\rho_f\left(\frac{\partial\overline{V}}{\partial\bar{t}} + \overline{U}\frac{\partial\overline{V}}{\partial\overline{X}} + \overline{V}\frac{\partial\overline{V}}{\partial\overline{Y}}\right) = -\frac{\partial\overline{P}}{\partial\overline{Y}} + \left(\mu + \frac{1}{\beta c^*}\right)$$
$$\left(\frac{\partial^2\overline{V}}{\partial\overline{X}^2} + \frac{\partial^2\overline{V}}{\partial\overline{Y}^2}\right) - \frac{1}{2\beta c^{*3}}\left(\frac{\partial\overline{V}}{\partial\overline{X}} + \frac{\partial\overline{V}}{\partial\overline{Y}}\right)^2\left(\frac{\partial^2\overline{V}}{\partial\overline{X}^2} + \frac{\partial^2\overline{V}}{\partial\overline{Y}^2}\right) \tag{2.7}$$

Energy Equation:

$$(\rho c)_f\left(\frac{\partial\overline{T}}{\partial\bar{t}} + \overline{U}\frac{\partial\overline{T}}{\partial\overline{X}} + \overline{V}\frac{\partial\overline{T}}{\partial\overline{Y}}\right) = K_T\left(\frac{\partial^2\overline{T}}{\partial\overline{X}^2} + \frac{\partial^2\overline{T}}{\partial\overline{Y}^2}\right) + (\rho c)_p$$
$$\left[D_B\left(\frac{\partial\overline{C}}{\partial\overline{X}}\frac{\partial\overline{T}}{\partial\overline{X}} + \frac{\partial\overline{C}}{\partial\overline{Y}}\frac{\partial\overline{T}}{\partial\overline{Y}}\right) + \frac{D_T}{T_m}\left(\left(\frac{\partial\overline{T}}{\partial\overline{X}}\right)^2 + \left(\frac{\partial\overline{T}}{\partial\overline{Y}}\right)^2\right)\right]$$
$$-\left(\frac{\partial\overline{q_r}}{\partial\overline{X}} + \frac{\partial\overline{q_r}}{\partial\overline{Y}}\right) \tag{2.8}$$

Concentration Equation:

$$\left(\frac{\partial\overline{C}}{\partial\bar{t}} + \overline{U}\frac{\partial\overline{C}}{\partial\overline{X}} + \overline{V}\frac{\partial\overline{C}}{\partial\overline{Y}}\right) = D_B\left(\frac{\partial^2\overline{C}}{\partial\overline{X}^2} + \frac{\partial^2\overline{C}}{\partial\overline{Y}^2}\right) +$$
$$\frac{D_T}{T_m}\left(\frac{\partial^2\overline{T}}{\partial\overline{X}^2} + \frac{\partial^2\overline{T}}{\partial\overline{Y}^2}\right) \tag{2.9}$$

where ρ_f is fluid density, β_T is coefficient of thermal expansion, $\overline{P}$ is pressure, q_r is radiative heat flux, E_x is axially applied electric field, T_m is fluid mean temperature, g is acceleration due to gravity, ρ_p is particle density, $(\rho c)_p$ is heat capacity of the material, β_c is coefficient of concentration expansion, K_T is thermal conductivity of nanofluids , $\overline{T}$ is nanoparticle temperature, D_B is coefficient of Brownian diffusion, $\overline{C}$ is nanoparticle concentration, D_T is thermophoretic diffusion coefficient, $(\rho c)_f$ is heat capacity of fluid.

Compare to $\overline{Y}$ direction, radiative heat flux along $\overline{X}$ -direction is regarded insignificant. Therefore, q_r is determined by applying Rosseland assumption [18].

$$q_r = -\frac{16\sigma^* T_0^3}{3k^*}\frac{\partial\overline{T}}{\partial\overline{Y}} \tag{2.10}$$

where k^* and σ^* stand for the mean absorption coefficient and the Stefan-Boltzman constant, respectively. The following is a expression for the Poisson Boltzmann equation regarding the distribution of electric potential that formed as a result of the electrical Debye layer, or EDL:

$$\nabla^2\overline{E} = -\frac{\overline{\rho_e}}{\varepsilon} \tag{2.11}$$

where $\overline{E}$ is the electric potential, $\overline{\rho_e} = ez(n^+ + n^-)$ stands for electrical charge density, ε is permittivity.

Introducing the relations between the laboratory and wave frame as

$$\bar{x} = \overline{X} - c\bar{t},\ \bar{y} = \overline{Y},\ \bar{u} = \overline{U} - c,\ \bar{v} = \overline{V}$$

Now, the non-dimensional terms can be put in the following form:

$$x = \frac{\bar{x}}{\lambda}, y = \frac{\bar{y}}{d}, X = \frac{\overline{X}}{\lambda}, Y = \frac{\overline{Y}}{d}, t = \frac{c\bar{t}}{\lambda}, v = \frac{\bar{v}}{c}, \delta = \frac{d}{\lambda},$$
$$u = \frac{\bar{u}}{c}, p = \frac{d^2\bar{p}}{c\lambda\mu}, Pr = \frac{\mu}{\alpha}, \alpha = \frac{K_T}{(\rho c)_f}, \theta = \frac{\overline{T} - \overline{T}_0}{\overline{T}_1 - \overline{T}_0},$$
$$\sigma = \frac{\overline{C} - \overline{C}_0}{\overline{C}_1 - \overline{C}_0}, Uhs = \frac{-E_x\varepsilon\xi}{\mu c}, E = \frac{\overline{E}}{\xi}, Nt = \frac{(\rho c)_p D_T(\overline{T}_1 - \overline{T}_0)}{(\rho c)_f \mu T_m},$$
$$Gr = \frac{\rho_f g d^2(\overline{T}_1 - \overline{T}_0)\beta_T}{c\mu}, Nb = \frac{(\rho c)_p D_B(\overline{C}_1 - \overline{C}_0)}{(\rho c)_f \mu},$$
$$Rn = \frac{16\sigma^* T_0^3}{3k^*\mu c_f}, \mathrm{R} = \frac{\rho_f c d}{\mu}, \nabla^2\overline{E} = -\frac{\overline{\rho_e}}{\varepsilon},$$

$$B_r=\frac{(\rho_p-\rho_f)gd^2(\overline{C_1}-\overline{C_0})\beta_c}{c\mu},q_r=-\frac{16\sigma^* T_0^3}{3k*}\frac{\partial\overline{T}}{\partial\overline{Y}} \tag{2.12}$$

where A and B are the dimensionless Eyring-Powell fluid parameters, p is dimensionless pressure, Pr is Prandtl number, θ is dimensionless temperature, δ is wave number, σ is dimensionless nanoparticle volume fraction, k is electro-osmosis parameter, Uhs is Helmholtz-Smoluchowski velocity, Nt is thermophoresis parameter, Gr is local temperature Grashof number, Nb is Brownian motion parameter, Rn is thermal radiation parameter, B_r is local nanoparticle Grashof number, R is Reynold's number. Considering approach Debye-Huckel linearization, (i.e. $\sinh\left(\frac{ezE}{K_BT}\right)\approx\frac{ezE}{K_BT}$) and imposing the boundary conditions $E=0$ at $y=h_1$ and $E=1$ at $y=h_2$, the potential function is obtained as: $E=\frac{\sinh(k(y-h_1))}{\sinh(k(h_2-h_1))}$, where $k=deZ\sqrt{\frac{2n_0}{\varepsilon K_BT_e}}=\frac{a}{\lambda_d}$, λ_d is Debye length of EDL.

The governing equations possess the following forms after non-dimensionalizing Eqs. (2.6) to (2.11) and expressing the velocity components in terms of stream functions $\left(u=\frac{\partial\psi}{\partial y},v=-\delta\frac{\partial\psi}{\partial x}\right)$ with low Reynolds numbers as well as long wavelengths assumptions.

$$0=-\frac{\partial p}{\partial x}+(1+B)\frac{\partial^3\psi}{\partial y^3}-A\left(\frac{\partial^2\psi}{\partial y^2}\right)^2\frac{\partial^3\psi}{\partial y^3}+k^2UhsE$$
$$+Gr\theta+B_r\sigma \tag{2.13}$$

$$\frac{\partial p}{\partial y}=0 \tag{2.14}$$

$$\left(\frac{1+Rn\Pr}{\Pr}\right)\frac{\partial^2\theta}{\partial y^2}+Nb\frac{\partial\sigma}{\partial y}\frac{\partial\theta}{\partial y}+Nt\left(\frac{\partial\theta}{\partial y}\right)^2=0 \tag{2.15}$$

$$\frac{\partial^2\sigma}{\partial y^2}+\frac{Nt}{Nb}\frac{\partial^2\theta}{\partial y^2}=0 \tag{2.16}$$

Differentiating Eqn.(2.13) with respect to y, we have

$$(1+B)\frac{\partial^4\psi}{\partial y^4}-A\frac{\partial}{\partial y}\left[\left(\frac{\partial^2\psi}{\partial y^2}\right)^2\frac{\partial^3\psi}{\partial y^3}\right]+k^2Uhs\frac{\partial E}{\partial y}+$$
$$Gr\frac{\partial\theta}{\partial y}+B_r\frac{\partial\sigma}{\partial y}=0 \tag{2.17}$$

The suitable boundary conditions are as follows:

$\psi=-\frac{F_l}{2},\frac{\partial\psi}{\partial y}=0,\theta=0$ and $\sigma=0$ at

$$y=h_1=-1-mx-a\sin(2\pi(x-t)+\phi) \tag{2.18}$$

$\psi=\frac{F_l}{2},\frac{\partial\psi}{\partial y}=0,\theta=1$ and $\sigma=1$ at

$$y=h_2=1+mx+b\sin(2\pi(x-t)) \tag{2.19}$$

The instantaneous volume rate of the flow $F_l(x,t)$ can be derived as:

$$F_l(x,t)=\Theta+a\sin(2\pi(x-t)+\phi)+b\sin(2\pi(x-t)) \tag{2.20}$$

where $F_l=\frac{\overline{Q}}{ca},\Theta=\frac{\overline{q}}{ca},F_l=\int_{h_1}^{h_2}udy=\psi(h_2-h_1)$ and Θ is the mean time rate of the flow.

3. SOLUTION OF THE PROBLEM

By employing Homotopy Perturbation Sumudu Transformation approach, partial differential Equations (2.15)-(2.17) are solved to find analytical solutions with boundary conditions (2.18)-(2.19).

$$\psi(y)=p+qy+r\frac{y^2}{2}+s\frac{y^3}{6}+\frac{v^4}{1+B}S^{-1}$$
$$\left[S\left(A\frac{\partial}{\partial y}\left[\left(\frac{\partial^2\psi}{\partial y^2}\right)^2\frac{\partial^3\psi}{\partial y^3}\right]-k^2Uhs\frac{\partial E}{\partial y}-Gr\frac{\partial\theta}{\partial y}-B_r\frac{\partial\sigma}{\partial y}\right)\right]$$

$$\theta(y)=e+fy-\left(\frac{\Pr}{1+Rn\Pr}\right)$$
$$S^{-1}\left[v^2S\left(Nb\frac{\partial\sigma}{\partial y}\frac{\partial\theta}{\partial y}+Nt\left(\frac{\partial\theta}{\partial y}\right)^2\right)\right]$$

$$\sigma(y)=h+gy-\frac{Nt}{Nb}S^{-1}\left[v^2S\left(\frac{\partial^2\theta}{\partial y^2}\right)\right]$$

here p,q,r,s,e,f,g and h are constants to be obtained by using boundary conditions (2.18)-(2.19).

4. RESULTS AND DISCUSSION

The present analysis shows a graphical representation of how temperature, velocity and nanoparticle volume fraction vary with the relevant parameters by using MATHEMATICA software and the effects were discussed in brief.

4.1: Velocity Profile

Fig.2(a) to Fig.2(f) illustrate how various parameters affect velocity. Fig.2(a) and Fig.2(b) indicate how fluid parameters A and B affect velocity respectively. Since fluid parameters and viscosity of the fluid are inversely related, we can observe that when the Eyring-Powell fluid parameter increases, the fluid's velocity u decreases. Fig.2(c) shows how velocity is affected by electro-osmotic parameter k. The findings reveal that velocity curve behaves differently at centre and close to the channel walls. The velocity initially rises with electro-osmotic parameter k (when electro-osmotic driving force dominates) but then reduces at larger k (EDL becomes too thin and electro-osmotic pumping weakens in the core). The variation of velocity with Helmholtz-Smoluchowski velocity Uhs is depicted in Fig.2(d). The non-dimensional velocity is observed to decrease as Helmholtz-Smoluchowski velocity Uhs increases. Fig.2(e) and Fig.2(f) represent how velocity varies corresponding to the changes in the values of local temperature Grashof number Gr along with the local nanoparticle Grashof number B_r respectively. We can examine that with rise in the local temperature Grashof number Gr, velocity close to the walls reduces, while centreline velocity enhances. This is attributed to the competing effects of viscous drag and buoyancy forces: at the walls viscous resistance dominates, whereas in the core region buoyancy accelerates the fluid, resulting in enhanced velocity at higher Gr. Identical behaviour is inspected for the local nanoparticle Grashof number B_r.

4.2: Temperature and nanoparticle volume fraction Profile

Fig.3(a) to Fig.3(d) show how various parameters affect variation of temperature and the nanoparticle volume fraction. Fig. 3(a) illustrates how variation of temperature and nanoparticle volume fraction occurs on changing the Prandtl number Pr. It demonstrates that as the Prandtl number Pr rises, the temperature rises as well, but the volume fraction of nanoparticles falls. Fig.3(b) illustrates how thermal radiation parameter Rn affects variation of temperature and the volume fraction of nanoparticles. It demonstrates that with increasing in thermal radiation parameter Rn, nanoparticle volume fraction rises, but the temperature declines as it does. Fig.3(c) illustrates how nanoparticle volume fraction and temperature variations are affected by Brownian motion parameter Nb. Clearly, nanoparticle volume fraction enhances when the Brownian motion parameter Nb increases and same observation is made in case of temperature also. Fig.3(d) illustrates how volume fraction of nanoparticles and temperature variations are affected by thermophoresis parameter Nt. It demonstrates that with increase in the thermophoresis parameter Nt, the temperature rises, yet the nanoparticle volume fraction decreases as the value rises.

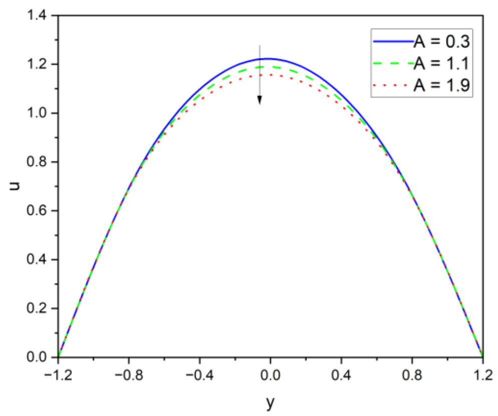

Fig.2(a) Variation of velocity with A

when $a = 0.1$, $b = 0.5$, $m = 0.2$, $\phi = \pi$, $t = 0.5$, $x = 1$, $\Theta = 1.7$, $k = 1$, $Uhs = -2$, $Gr = 0.5$, $B_r = 0.6$, $B = 1$

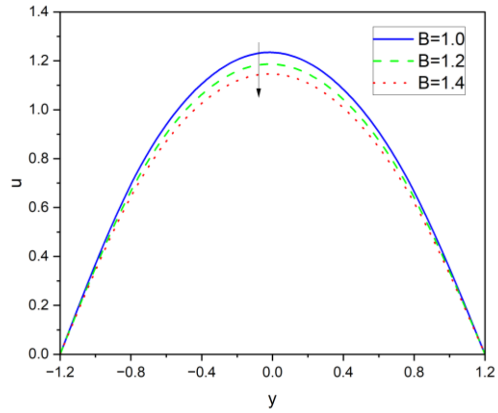

Fig.2(b) Variation of velocity with B

when $a = 0.1,\ b = 0.5,\ m = 0.2,\ \phi = \pi,\ t = 0.5,\ x = 1,\ \Theta = 1.7,\ k = 1,\ Uhs = -2,\ Gr = 0.5,\ B_r = 0.6,\ A = 0.004$

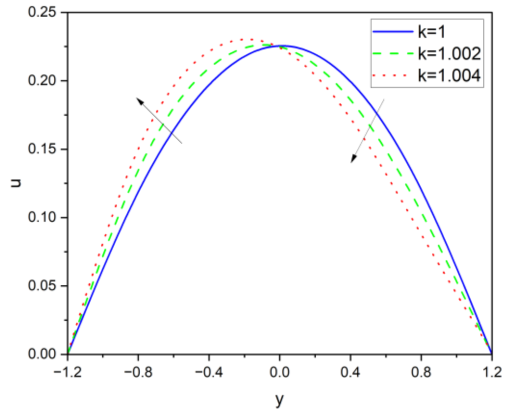

Fig.2(c) Variation of velocity with k

when $a = 0.1,\ b = 0.5,\ m = 0.2,\ \phi = \pi,\ t = 0.5,\ x = 1,\ \Theta = 1.7,\ Uhs = -1,\ Gr = 0.5,\ B_r = 0.5,\ A = 0.0001,\ B = 1.2,$ $Pr = 0.6,\ Nt = 0.3,\ Nb = 0.1,\ Rn = 2$

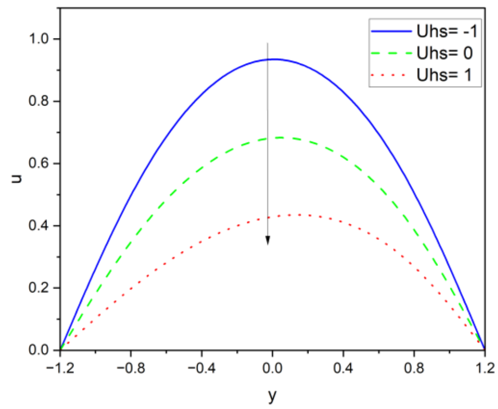

Fig.2(d) Variation of velocity with Uhs

when $a = 0.1,\ b = 0.5,\ m = 0.2,\ \phi = \pi,\ t = 0.5,\ x = 1,\ \Theta = 1.7,\ k = 1,\ Gr = 0.5,\ B_r = 0.6,\ A = 0.004,\ B = 1$

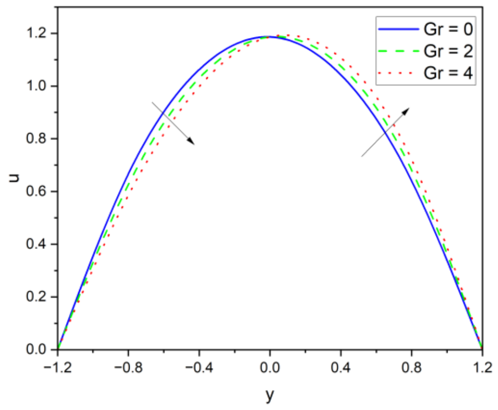

Fig.2(e) Variation of velocity with Gr

when $a = 0.1$, $b = 0.5$, $m = 0.2$, $\phi = \pi$, $t = 0.5$, $x = 1$, $\Theta = 1.7$, $k = 1$, $Uhs = -2$, $B_r = 1.1$, $A = 0.004$, $B = 1.2$

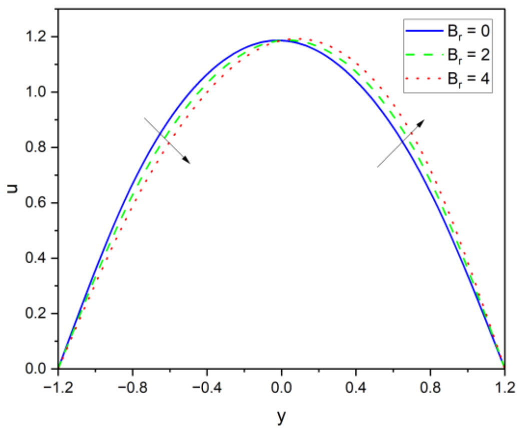

Fig.2(f) Variation of velocity with B_r

when $a = 0.1$, $b = 0.5$, $m = 0.2$, $\phi = \pi$, $t = 0.5$, $x = 1$, $\Theta = 1.7$, $k = 1$, $Uhs = -2$, $Gr = 1$, $A = 0.004$, $B = 1.2$

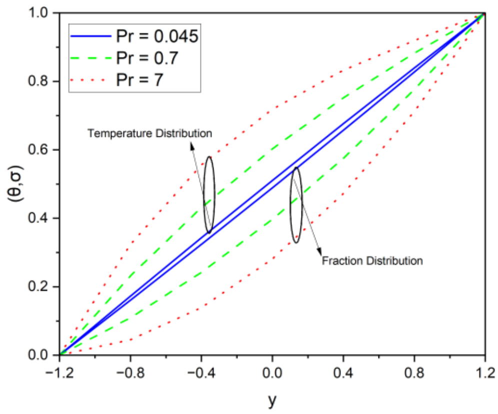

Fig.3(a) Variation of nanoparticle volume fraction and temperature with Pr

when $a = 0.1$, $b = 0.5$, $m = 0.2$, $\phi = \pi$, $t = 0.5$, $x = 1$, $Rn = 1$, $Nt = 1$, $Nb = 1$

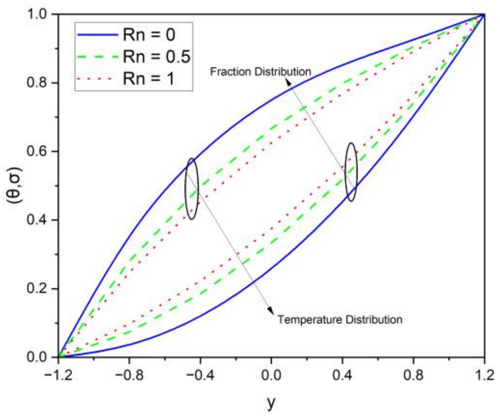

Fig.3(b) Variation of nanoparticle volume fraction and temperature with *Rn*

when $a = 0.1,\ b = 0.5,\ m = 0.2,\ \phi = \pi\ ,\ t = 0.5,\ x = 1,\ Pr = 1,\ Nt = 1,\ Nb = 1$

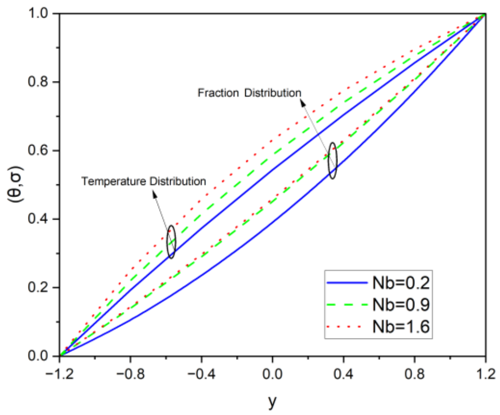

Fig.3(c) Variation of nanoparticle volume fraction and temperature with *Nb*

when $a = 0.1,\ b = 0.5,\ m = 0.2,\ \phi = \pi\ ,\ t = 0.5,\ x = 1,\ Pr = 1,\ Nt = 0.5,\ Rn = 1$

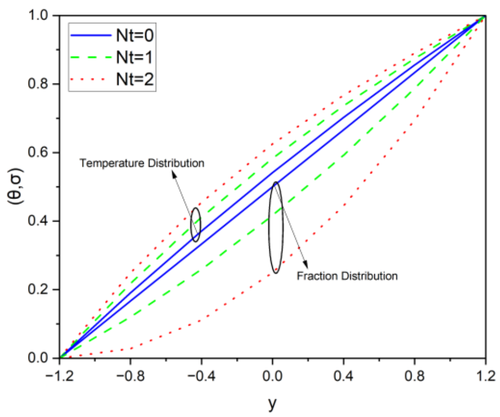

Fig.3(d) Variation of nanoparticle volume fraction and temperature with *Nt*

when $a = 0.1,\ b = 0.5,\ m = 0.2,\ \phi = \pi\ ,\ t = 0.5,\ x = 1,\ Pr = 0.5,\ Nb = 1,\ Rn = 1$

5. CONCLUDING REMARKS

The influence of thermal radiation on electro-osmosis modulated the peristaltic transport of an Eyring-Powell non-Newtonian fluid through tapered asymmetric channel has been examined in this research. The following are the key outcomes of the current analysis:

- Velocity tends to reduce with increase in A and B.
- The velocity first enhances with the electro-osmotic parameter k, but then begins to decline after the centerline.
- Velocity profile decreases as Helmholtz-Smoluchowski velocity Uhs increases.
- The velocity profile exhibits a similar behaviour for Gr and B_r.
- When Nb, Pr and Nt increase, then temperature also increases.
- Temperature reduces with rise in the thermal radiation effects.
- As the Prandtl number Pr as well as thermophoresis effects increase, the volume fraction of nanoparticles decreases.
- With rise in Rn and Nb, the volume fraction of nanoparticles increases as well.

AUTHOR CONTRIBUTIONS: Conceptualization, analysis and supervision work performed by the author Asha S. Kotnurkar. Literature survey, modeling, methodology, software handling, writing-original draft prepared by the author Susama Junjappanavar. All authors equally contributed to the study and all authors read, commented and approved the final manuscript.

FUNDING: No external funding is received for conducting this study.

DATA AVAILABILITY: All data generated or analyzed during this study are included in this published article.

AUTHORS' DECLARATION: We hereby confirm that all the Figures in the manuscript are ours.

COMPETING INTERESTS: The authors declare no competing interests.

ETHICS, CONSENT TO PARTICIPATE AND CONSENT TO PUBLISH DECLARATIONS: Not Applicable

REFERENCES

[1] S. K. Asha, and G. Sunitha. "Mixed convection peristaltic flow of a Eyring–Powell nanofluid with magnetic field in a non-uniform channel." *Journal of Applied Mathematics and Computation* 2.8 (2018): 332-334.

[2] T. W. Latham. *Fluid motion in a peristaltic pump.* M.S. Thesis, M.I.T., Cambridge. (1966).

[3] S. K. Asha, and G. Sunitha. "Peristaltic transport of Eyring–Powell nanofluid in a non-uniform channel." *Jordan Journal of Mathematics and Statistics* 12.3 (2019): 431-453.

[4] A. H. Shapiro, M. Y. Jaffrin, and S. L. Weinberg. "Peristaltic pumping with long wavelengths at low Reynolds number." *Journal of Fluid Mechanics* 37.4 (1969): 799-825.

[5] M. Y. Jaffrin, and A. H. Shapiro. "Peristaltic pumping." *Annual Review of Fluid Mechanics* 3 (1971): 13-37.

[6] S. K. Asha, and N. Kallolikar. "Thermal analysis for peristaltic flow of nanofluid under the influence of porous medium and double diffusion in non-uniform channel using Sumudu Transformation Method." *Annals of Pure and Applied Mathematics* 23.2 (2021): 73-91.

[7] S. K. Asha, and G. Sunitha. "Influence of thermal radiation on peristaltic blood flow of a Jeffrey fluid with double diffusion in the presence of gold nanoparticles." *Informatics in Medicine Unlocked* 17 (2019): 100272.

[8] A. Ali, Y. Ali, D. N. Khan Marwat, M. Awais, and Z. Shah. "Peristaltic flow of nanofluid in a deformable channel with double diffusion." *SN Applied Sciences* 2.1 (2020): 1-10.

[9] S. K. Asha, and N. Kallolikar. "Effect of surface roughness and induced magnetic field on electro-osmosis peristaltic flow of Eyring-Powell nanofluid in a tapered asymmetric channel." *Journal of Advanced Research in Numerical Heat Transfer* 10.1 (2022): 20-37.

[10] A. Tanveer, S. Mahmood, T. Hayat, and A. Alsaedi. "On electroosmosis in peristaltic activity of MHD non-Newtonian fluid." *Alexandria Engineering Journal* 60.3 (2021): 3369-3377.

[11] P. Jayavel, R. Jhorar, D. Tripathi, and M. N. Azese. "Electroosmotic flow of pseudoplastic nanoliquids via peristaltic pumping." *Journal of the Brazilian Society of Mechanical Sciences and Engineering* 41.2 (2019): 1-18.

[12] M. K. Chaube, A. Yadav, D. Tripathi, and O. A. Bég. "Electroosmotic flow of biorheological micropolar fluids through microfluidic channels." *Korea-Australia Rheology Journal* 30.2 (2018): 89-98.

[13] R. E. Powell, and H. Eyring. "Mechanism for the relaxation theory of viscosity." *Nature* 154 (1944): 427-428.

[14] F. M. Abbasi, A. Alsaedi, and T. Hayat. "Peristaltic transport of Eyring-Powell fluid in a curved channel." *Journal of Aerospace Engineering* 27.6 (2014).

[15] K. Vajravelu, and K. V. Prasad. "Heat transfer phenomena in a moving nanofluid over a horizontal surface." *Journal of Mechanics* 28.3 (2012): 579-588.

[16] J. Prakash, A. Sharma, and D. Tripathi. "Thermal radiation effects on electroosmosis modulated peristaltic transport of ionic nanoliquids in biomicrofluidics channel." *Journal of Molecular Liquids* 249 (2018): 843-855.

[17] S. K. Asha, and G. Sunitha. "Effect of joule heating and MHD on peristaltic blood flow of Eyring–Powell nanofluid in a non-uniform channel." *Journal of Taibah University for Science* 13.1 (2019): 155-168.

[18] M. Kothandapani, and J. Prakash. "Influence of heat source, thermal radiation, and inclined magnetic field on peristaltic flow of a hyperbolic tangent nanofluid in a tapered asymmetric channel." *IEEE Transactions on Nanobioscience* 14.4 (2015): 385-392.